Asymptotic Behavior of the Rayleigh-Taylor Instability

Laurent Duchemin,[1] Christophe Josserand,[2] and Paul Clavin[3]

[1]*Department of Applied Mathematics and Theoretical Physics, University of Cambridge, Cambridge CB3 0WA, United Kingdom*
[2]*Laboratoire de Modélisation en Mécanique, UPMC-CNRS UMR 7607, 4 place Jussieu, 75252 Paris CEDEX 05, France*
[3]*IRPHE, Universités d'Aix-Marseille I and II-CNRS, 49 rue Joliot-Curie, BP 146, 13384 Marseille CEDEX, France*

(Received 19 December 2004; published 8 June 2005)

We investigate long time numerical simulations of the inviscid Rayleigh-Taylor instability at Atwood number one using a boundary integral method. We are able to attain the asymptotic behavior for the spikes predicted by Clavin and Williams for which we give a simplified demonstration. In particular, we observe that the spike's curvature evolves as t^3, while the overshoot in acceleration shows good agreement with the suggested $1/t^5$ law. Moreover, we obtain consistent results for the prefactor coefficients of the asymptotic laws. Eventually we exhibit the self-similar behavior of the interface profile near the spike.

DOI: 10.1103/PhysRevLett.94.224501 PACS numbers: 47.20.Ma, 47.11.+j, 47.20.Ky

Introduction.—The Rayleigh-Taylor (RT) instability appears when, under gravity, a heavy liquid is placed over a lighter one [1]. This instability is crucial for our understanding of different phenomena in fluid mechanics: mixing, thermal convection ([2], and references therein), and also finger number selection in splashes [3]. It is also important in inertial confinement fusion (ICF) where the mass ablation provides a stabilizing effect to the interface instability [4]. Without ablation, after the exponential growth of the perturbations due to the linear RT instability, nonlinear profiles develop through the formation of bubbles of lighter fluid rising into the heavier one and falling spikes of the heavier liquid penetrating the lighter one. In the general situations of viscous fluids, which are immiscible and/or have Atwood number not equal to unity [$A_T = (\rho_h - \rho_l)/(\rho_h + \rho_l)$, with ρ_h and ρ_l being the density of the heavier and lighter fluids, respectively], famous mushroomlike structures grow for larger times [2,5,6]. The limit of an inviscid fluid above a vacuum ($A_T = 1$) without surface tension plays a specific role since no stabilizing effects are present in the linear dynamics. It is important to understand ICF in the limit of high density ratio, and it is also the most challenging case for the numerics. Most theoretical and numerical work have focused on this idealized limit in order to track insights into the instability itself [7–12]. It has been shown using a conformal mapping that a finite time singularity might appear in the conformal plane [13], and it is also suspected that for some sufficiently irregular initial conditions finite time singularities should also be observed in the physical plane. However, starting with sufficiently smooth initial conditions, the asymptotic dynamics [8,11,12] presents a constant velocity rising bubble separated by free falling tiny spikes as displayed in Fig. 1. Although the rising bubble motion has been described using local properties of the flow [14], the asymptotic dynamics of the spikes is far from being well understood. The single mode approach gives a fair description of the constant velocity of the rising bubble [$v_b = \sqrt{g/(3k)}$, where g is the acceleration of the gravity and k the wave number of the perturbation] but gives only partial results for the spike [8]. The fluid there obeys free fall dynamics to a good approximation, and the pressure field of the flow leads to an overshoot in the acceleration. The accelerated motion of the liquid stretches the spike geometry and one expects self-similar behavior of the tip of the spikes.

Recently, an asymptotic theory using a parallel flow description of the velocity field near the spikes has been constructed [15]. The interface dynamics is nonlinear for large time and can be described using the theory of characteristics which gives rise to finite time singularity solutions. In the case of regular dynamics, a self-similar description of the peak is obtained for large time: the maximal curvature of the interface at the peak tip is found to behave as the cubic power of time t^3. Moreover, the

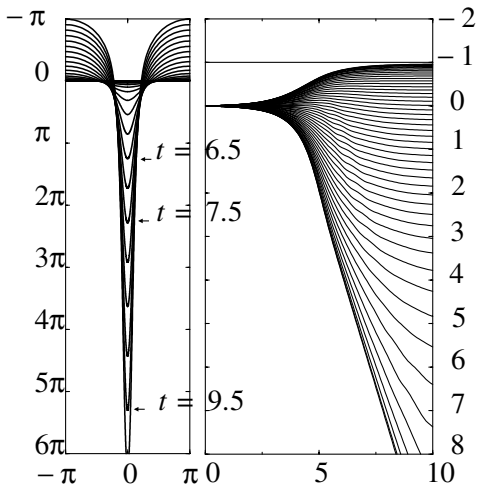

FIG. 1. Snapshots of the interface subject to the Rayleigh-Taylor instability for time ranging from $t = 0$ to 10, starting with a small amplitude sine mode (left). On the right is shown the velocity of several points along the interface, nondimensionalized with the stationary bubble rising velocity $\sqrt{g/3k}$, as a function of time.

spike position, following the free fall $\frac{1}{2}gt^2$ at leading order, is shown to converge to the constant acceleration g with an overshoot in acceleration decreasing as t^{-5}. In this Letter, we present a numerical study of the Rayleigh-Taylor instability which focuses on the large time dynamics of the spikes in order to investigate the self-similar dynamics predicted in [15], where no numerical studies were performed. We consider the dynamics for an inviscid liquid (heavy) with an exterior fluid of zero density ($A_t = 1$) and no surface tension. The numerics use a boundary integral method. Because of strong numerical instabilities, a careful treatment of the interface using conformal mapping is needed as explained below. The results are then shown and compared with the theory.

Asymptotic analysis and numerical method.—We consider the two-dimensional motion of an inviscid fluid above a vacuum, subject to a negative acceleration $-g$. A periodic sine perturbation of the interface of wave number k is implemented as initial conditions. Neglecting surface tension, the equations of motion have no control parameter after rescaling the time, the position, and the velocity potential φ by factors $\sqrt{gk}$, k, and $\sqrt{k^3/g}$, respectively. The interface is described by $y = \alpha(x, t)$, where y is the direction along the gravity and x orthogonal to it (see Fig. 2). The velocity field $\mathbf{U} = (u, v)$ satisfies the dimensionless Euler equation

$$\frac{d\mathbf{U}}{dt} = -\nabla P + \mathbf{e_y},$$

where $P(x, y, t)$ is the pressure, $\mathbf{e_y}$ the nondimensional acceleration due to gravity, and the fluid density $\rho = 1$. The kinetic equation for the interface reads

$$\frac{\partial \alpha(x, t)}{\partial t} + u\frac{\partial \alpha(x, t)}{\partial x} = v,$$

with the velocity field (u, v) evaluated at the interface $[x, \alpha(x, t)]$. Starting at time $t = 0$ with a small sine amplitude interface, we observe for large time that the fluid particles located in the vicinity of the tiny spikes come from an almost free fall from the initial interface region. Therefore, following [15], we assume quasiparallel steady flow for the velocity field which gives then in the tip region $|u| \ll |v|$ and $v \sim \sqrt{2y}$ with $y \sim \frac{1}{2}t^2$ for large time. Writing a perturbation expansion of the velocity field in the tip region $|x| \ll y$, we in fact consider $v = \sqrt{2[y + f(x, y, t)]}$, with $f(x, y, t) \ll y$. Taking a Taylor expansion in x of the perturbation f, we obtain by symmetry $v = \sqrt{2y} + \frac{f_0(y,t)}{\sqrt{2y}} + \frac{x^2}{2}\frac{f_2(y,t)}{\sqrt{2y}} + O(x^4)$. We limit our expansion to the second order in x for the velocity field later on. Incompressibility gives $u = -(\sqrt{\frac{1}{2y}} + \frac{\partial(f_0(y,t)/\sqrt{2y})}{\partial y})x + O(x^3)$. At the leading order [where we neglect even the perturbation $f(x, y, t)$], we obtain the following expression for the interface location:

$$\frac{\partial \alpha(x, t)}{\partial t} - \frac{x}{\sqrt{2\alpha(x, t)}}\frac{\partial \alpha(x, t)}{\partial x} = \sqrt{2\alpha(x, t)},$$

which can be solved using the methods of characteristics (see [15]). Writing $\alpha(x, t) = t[\frac{t}{2} - \gamma(x, t)]$ and noting that $\gamma(x, t) \ll t/2$ in the spike region, we obtain, after linearization,

$$\frac{\partial \gamma(x, t)}{\partial t} - \frac{x}{t}\frac{\partial \gamma(x, t)}{\partial x} = 0,$$

which has the self-similar solution of the form $\gamma(x, t) = \theta(xt)$. A first conclusion can be drawn about the curvature of the interface at the tip, $\kappa = -\partial^2\alpha/\partial x^2|_{x=0}$, which is thus found to increase as the cubic power of time [16]:

$$\kappa = t^3\theta''(0). \tag{1}$$

The next order terms of the expansion allow the determination of the function $f_0(y, t)$ near the tip. Using the constant value of the pressure at the interface, we use the projection of the Euler equation at the interface on its local tangent: $\frac{du}{dt} + \frac{\partial \alpha(x,t)}{\partial x}\frac{dv}{dt} = \frac{\partial \alpha(x,t)}{\partial x}$, since on the interface $dP(x, \alpha(x, t), t)/dx = 0$. We develop this equation at first nonzero order (which will end up the first order in x) with the expansion $\theta(xt) = \theta(0) + x^2t^2\theta''(0)/2 + O(x^4)$. Remembering that $|f| \ll y$, we can neglect also the large scale terms $\partial^2(f_0(y, t)/\sqrt{2y})/\partial t\partial y$ and $\sqrt{2y}\partial^2(f_0(y, t)/\sqrt{2y})/\partial y^2$ with respect to the others. We finally obtain for the tip position $y = y_s$: $\frac{\partial f_0(y_s,t)}{\partial t} + \sqrt{2y_s}\frac{\partial f_0(y_s,t)}{\partial y} = \frac{df_0(y_s,t)}{dt} = \sqrt{\frac{2}{y_s}}\frac{1}{\kappa}$.

Recalling that $\frac{dy_s}{dt} = \sqrt{2y_s} + \frac{f_0(y_s,t)}{\sqrt{2y_s}}$, we obtain, for the tip acceleration at leading order,

$$\frac{d^2y_s}{dt^2} = 1 + \frac{1}{\sqrt{2y_s}}\frac{df_0(y_s, t)}{dt} = 1 + \frac{2}{t^5\theta''(0)}, \tag{2}$$

which corresponds to an overshoot in the spike acceleration decreasing as the fifth power of time. An overshoot in the acceleration was observed in numerical simulation already in [17], but with no explicit scaling laws.

The numerical method is elaborated using the incompressible and potential properties of the flow. The velocity field can thus be evaluated everywhere when the velocity potential is known on the interface thanks to Cauchy's theorem, in the spirit of other pioneering works [17–20]. The nondimensional Bernoulli equation on the free surface

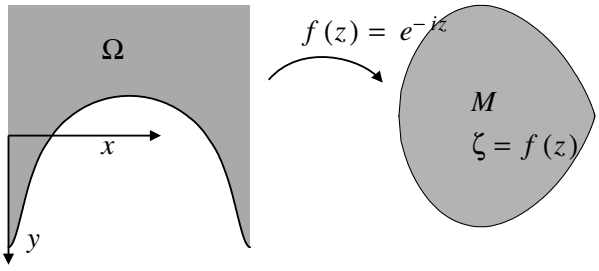

FIG. 2. Conformal map used to transform the physical periodic plane Ω into a closed domain M.

reads

$$\frac{\partial \varphi}{\partial t} = -\frac{1}{2}(\nabla \varphi)^2 + y, \tag{3}$$

where the velocity potential φ is a harmonic function in the fluid domain Ω:

$$\Delta \varphi = 0. \tag{4}$$

The kinematic condition on the free surface expresses the fact that fluid particles move with the same normal velocity as the free surface itself:

$$\frac{d\mathbf{x}}{dt} \cdot \mathbf{n} = \nabla \varphi \cdot \mathbf{n}. \tag{5}$$

Knowing φ on the free surface at a given time step, we search for the solution of Eq. (4) that satisfies this boundary condition (5). We use the complex potential $\beta(z) = \varphi + i\psi$ and the conformal map $f(z) = \exp(-iz)$ (cf. Fig. 2), where $z = x + iy$ and ψ is the stream function. The conformal map transforms the periodic domain Ω into the closed domain M. Since ψ is harmonic inside Ω, $\beta(z)$ is analytic inside Ω and therefore $\gamma(\zeta) = \beta(f(z))$ is analytic inside M. Using Cauchy's theorem, we obtain a Fredholm equation of the second kind for the stream function ψ, which is solved using discretization of the free surface ($\partial\Omega$ and thus ∂M). This linear system of equations is solved using a LU decomposition. Once we know ψ on each point on ∂M, the complex velocity of each marker in the physical plane is given by

$$\frac{d\beta}{dz} = u - iv, \tag{6}$$

where u and v are the horizontal and vertical velocities, respectively. This complex velocity is computed with a finite difference scheme using the values of the complex potential on the collocation points on $\partial\Omega$.

The position of the surface markers (kinematic condition) and the value of the velocity potential on each of these markers (Bernoulli equation) are then updated in time using a fourth order Runge-Kutta method. Finally, an adaptive mesh refinement technique is used in order to concentrate markers on the spike.

Results and discussions.—We have performed numerical simulations of the Rayleigh-Taylor instability using the numerical method described above. We start with a sine-mode deformation of the interface of amplitude $a \ll 1$. The unavoidable numerical noise cannot be damped by the numerics and the calculations always end up subject to numerical instabilities. Nevertheless, we emphasize that the numerical scheme used here is remarkably robust and can be accurately evolved to reach the large time where the scalings predicted by the theory [15] are valid. Comparing our simulations with recent numerical works [5,6,9], we have been able to run the dynamics at least twice as far, which corresponds roughly to an increase of a factor of 8 in the tip's curvature.

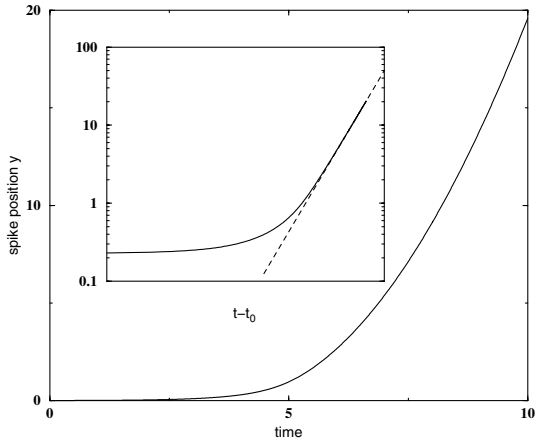

FIG. 3. Position of the spike $y_s(t)$ as a function of time. The inset shows in a log-log plot of the spike position (solid curve) as function of time $t - t_0$, with $t_0 = 3.74$ obtained by a second order polynomial fit of y_s. The dashed line shows the expected behavior $\frac{1}{2}t^2$.

The position of the spike is shown on Fig. 3 as function of time. We observe that the asymptotic dynamics are very well approximated by the relation $y_s = \frac{1}{2}g(t - t_0)^2$, as shown in the inset of the figure with $t_0 = 3.74$ for the amplitude of the initial perturbation $a = 0.01$. This remarkable behavior, in good agreement with the free fall hypothesis, suggests that t_0 is the time delay accounting for the initial exponential development of the instability. Indeed, the linear growth rate of the perturbation is precisely one, and, varying a, we observe that the time delay correspond to $ae^{t_0} = 0.42$, which corresponds in the numerical simulation to a constant amplitude of the spike of 0.22 to be compared to 0.21 obtained with the linear instability only. The time and amplitude correspond thus roughly to the transition between the linear and the nonlinear regime. We will therefore present further data on the curvature dependence and the acceleration of the tip as functions of this delayed time $t - t_0$ instead of t.

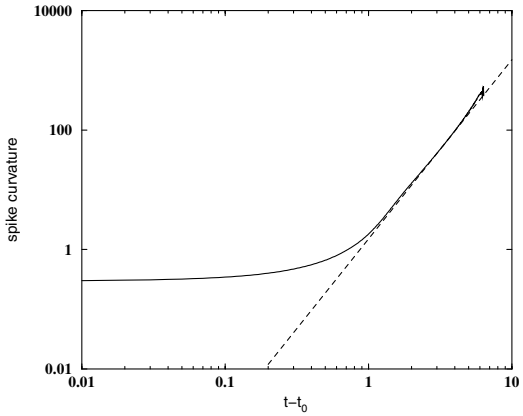

FIG. 4. Spike curvature κ_s calculated at the tip $y = y_s$ as function of the delayed time $t - t_0$ in a log-log plot. The dashed line displays the cubic law (1) with $\theta''(0) = 1.5$.

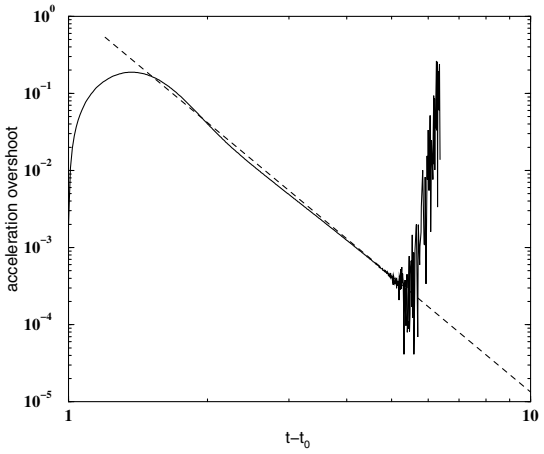

FIG. 5. Overshoot in acceleration, defined as the difference between the tip acceleration and the gravity. The plot is in log-log scale and with the delayed time $t - t_0$. The dashed line shows the theoretical prediction (2) using the value of $\theta''(0)$ obtained from Fig. 4.

The curvature κ_s at the tip is then shown in Fig. 4. The large time asymptotic behavior is similarly found to follow the cubic law [see Eq. (1)] with $\theta''(0) = 1.5$. We have not been able to deduce analytically this value of the self-similar curvature $\theta''(0) = 1.5$ using the characteristic dynamics, which is valid for large times only.

In addition, the acceleration of the tip is computed by finite differences on the tip velocity and the overshoot in the acceleration is presented on Fig. 5. We observe that the results look noisier than the two previous ones. Two factors can explain such noise: first, we are looking to a finite difference which decreases to zero so that the numerical errors are relatively more important. However, we note that the overshoot in acceleration shows good agreement with the $1/t^5$ law, noting that no adjustable parameter is used in this comparison. Finally, the self-similar structure of the interface near the tip has been exhibited on Fig. 6. We observe after the proper rescaling on the left part of the figure that the interface profiles collapse onto a single curve near the spike.

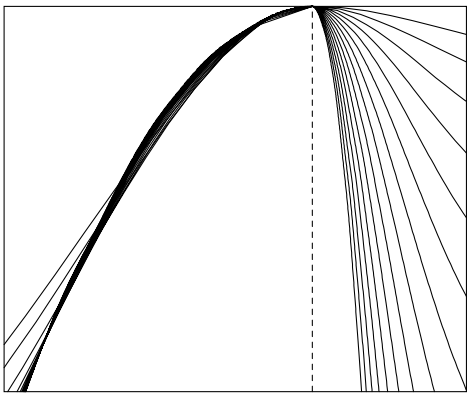

FIG. 6. Self-similar structure of the tip: the interface profiles around the spike have been superimposed on the right side of the figure for different time t ranging from 4 to 12. The left side of the figure shows the same curves rescaled by factor $1/(t - t_0)$ and $(t - t_0)$ for the x and y coordinates, respectively, following the scaling behavior predicted by the theory.

We have thus exhibited large times numerical simulations of the Rayleigh-Taylor instability which present asymptotic scaling behavior in agreement with theoretical predictions using Taylor expansions of the free fall velocity field at the spike [15]. Although our numerics always stops due to numerical instability, we have been able to reach large time enough to exhibit the cubic power in time dependence for the spike curvature and the inverse of the quintinc power of time decreasing of the overshoot in acceleration. Moreover, the numerical methods used here and the analytical description of the flow in the vicinity of the spike offer a powerful tool to investigate Rayleigh-Taylor and Richtmyer-Meshkov instabilities for any density ratio.

It is our pleasure to thank J. Ashmore for useful comments. We acknowledge also the support of CEA through Contract No. CEA/DIF N 4600051147/P6H29.

[1] Lord Rayleigh, *Scientific Papers II* (Cambridge University Press, Cambridge, UK, 1900), p. 200.
[2] B. Castaing, G. Gunaratne, F. Heslot, L. Kadanoff, A. Libchaber, S. Thomae, X. Wu, S. Zaleski, and G. Zanetti, J. Fluid Mech. **204**, 1 (1989).
[3] D. Gueyffier and S. Zaleski, C.R. Acad. Sci. Paris, Ser. IIb **326**, 839 (1998).
[4] J. Sanz, J. Ramirez, R. Ramis, R. Betti, and R. P. J. Town, Phys. Rev. Lett. **89**, 195002 (2002).
[5] S.-I. Sohn, Phys. Rev. E **67**, 026301 (2003).
[6] S.-I. Sohn, Phys. Rev. E **69**, 036703 (2004).
[7] D. Layzer, Astrophys. J. **122**, 1 (1955).
[8] Q. Zhang, Phys. Rev. Lett. **81**, 3391 (1998).
[9] G. Hazak, Phys. Rev. Lett. **76**, 4167 (1996).
[10] S. I. Abarzhi, Phys. Rev. Lett. **81**, 337 (1998).
[11] K. O. Mikaelian, Phys. Rev. Lett. **80**, 508 (1998).
[12] N. Inogamov, Astrophys. Space Phys. Rev. **10**, 1 (1999).
[13] S. Tanveer, Proc. R. Soc. A **441**, 501 (1993).
[14] V. N. Goncharov, Phys. Rev. Lett. **88**, 134502 (2002).
[15] P. Clavin and F. Williams, J. Fluid Mech. (to be published).
[16] It is interesting to notice that this cubic property is also found to be valid for the Richtmyer-Meshkov instability where the interface is only impulsively accelerated. There, the asymptotic vertical velocity field behaves as y/t near the spike, which is located around $y \sim v_0 t$. Numerical simulations are also found in correct agreement with this scaling.
[17] G. R. Baker, D. I. Meiron, and S. A. Orszag, Phys. Fluids **23**, 1485 (1980).
[18] T. Vinje and P. Brevig, Adv. Water Resour. **4**, 77 (1981).
[19] M. S. Longuet-Higgins and E. D. Cokelet, Proc. R. Soc. A **350**, 1 (1976).
[20] R. Menikoff and C. Zemach, J. Comput. Phys. **51**, 28 (1983).